Progress In Electromagnetics Research M, Vol. 71, 157–167, 2018

UHF Wave Propagation in Mine Shaft Environment

Shaohua Xue[1], Jianping Tan[1, 2, *], and Lixiang Shi[1]

Abstract—Wireless communication is very valuable in underground mines, in which channel characterization plays an important role. In this paper, both narrowband and wideband measurements at three typical ultra-high frequencies of 433, 900 and 2400 MHz in a real mine shaft are performed. To our knowledge, this is the first work focusing on radio propagation in the mine shaft environment. Important channel characteristics, such as the path loss, delay spread and the number of multipath components were extracted from the measured data and compared with that in tunnel channels. The effects of frequency and antenna position on the path loss were investigated. The relationship between the root-mean-square (RMS) delay spread and the transmitter-receiver distance was also analyzed. The results will deepen our understanding of the mine shaft channel and help to design shaft wireless systems.

1. INTRODUCTION

Reliable communication is of great importance in underground mines in terms of production management, transportation scheduling, miner's safety, condition motoring, and accident rescue. Underground mines are mainly composed of kilometers-long underground tunnels and hundreds- or kilometers-long mine shafts. Both of them are restricted space, which is a challenging environment for radio propagation because of high attenuation, multiple paths and electromagnetic interference [1]. In the past period of time, leaky feeder was considered a viable way to provide wireless service in such environments. However, leaky feeders were found unreliable in the case of landslide and fire because communication interruption may happen in the whole tunnel [2]. Wireless communication has been considered a must in such environments because its propagation medium is air. Nevertheless, wireless system performance largely depends on the channel characteristics, making it very necessary to study radio propagation in such environments [3].

There have been numerous studies on the radio propagation in underground tunnels or road/rail tunnels in the past decades. Some path loss models have been proposed, such as waveguide models [4], ray tracing models [5, 6], the numerical methods for solving Maxwell equations [7], and hybrid models [8, 9]. With the increase of communication rate, broadband communication systems are widely applied, even in tunnels. It makes wideband characteristics much more important now than before [10]. However, the above models mostly focus on the narrowband attenuation and do not perform well for wideband parameters, which are much more complex and largely depend on the physical environments. The experimental method is considered valuable [11]; nevertheless, they are more difficult to obtain due to the safety, cost, and permission issues. In [9], the path loss at 400 MHz in road and railway tunnels was measured. They found that the path loss could be divided into four segments: free space segment, high path loss segment (where the path loss is a linear function of the distance), waveguide segment and furthest segment (where the path loss is close to that in free space). In [12], the statistical

Received 4 June 2018, Accepted 1 August 2018, Scheduled 6 August 2018

* Corresponding author: Jianping Tan (jptan@csu.edu.cn).

[1] School of Mechanical and Electrical Engineering, Central South University, Changsha 410010, China. [2] State Key Laboratory of High Performance and Complex Manufacturing, Central South University, Changsha 410010, China.

characteristics in the underground mine tunnel and indoor corridor were compared. Both the path loss exponent and RMS delay spread were found smaller in the indoor corridor due to smoother surface and more regular cross-section. In [13], both narrowband and wideband measurements were conducted at 2.4 GHz in an underground mine tunnel. Results show that the received power has a greater variability when the Tx is closer to the sidewall, and the delay spread has a relatively small value in a long distance. In [14, 15], propagation measurements at 2.4 GHz, 5.8 GHz in underground mine tunnels were conducted, and the RMS delay spread was found to have almost no correlation with the distance, due to the arbitrary scattering paths caused by the very rough walls. In [16], the measurement results at 24 GHz in metropolitan railway tunnel show a small path loss exponent of 1.3, which means a clear waveguide effect. In addition, the delay spread decreases as the distance increases, highlighting that higher modes extinguish faster than the lower ones. In [17], a comparison of propagation at 980 MHz and 2.45 GHz in a subway tunnel was presented, indicating that the use of higher frequency can considerably reduce the multipath effect.

However, studies on radio propagation in the mine shaft environment have not been reported [18]. It partly leads to the lack of wireless service in mine cages, which is the base of voice calls, condition monitoring, and video surveillance. Thus, in this paper, the radio propagation in a real mine shaft is investigated at three widely used ultra-high frequencies of 433, 900, 2400 MHz. Important channel parameters such as path loss and delay spread are presented and compared with that in tunnels. The effect of antennas' positions on path loss was investigated. The relationship between delay spread and transmitter-receiver distance was also analyzed.

The paper is organized as follows: Section 2 describes the measurement setups; Section 3 presents and discusses the narrowband and wideband results extracted from the measured data; Section 4 concludes the paper.

2. MEASUREMENTS

2.1. Description of the Environment

In a mine shaft, the cage is dragged up and down by wire ropes to transport people, materials, and ores. There are some physical differences between mine shafts and underground mine tunnels or road/rail tunnels, which are presented in Table 1. It seems that mine shafts get a better physical condition for radio waves, in consideration of the line-of-sight (LOS) path and smooth walls (which reduce the roughness loss).

Table 1. Differences between mine shafts and underground mine tunnels or road/rail tunnels.

	Road/rail tunnels	**Underground mine tunnels**	**Mine shafts**
Cross-sections	Regular arched or rectangular	Irregular rectangular, circular, arched or trapezoid	Regular circular
Wall roughness	Small (several centimeters)	Large ($5 \sim 25$ cm)	Small (several centimeters)
Curvature	Straight or curved	Straight or curved	Straight
Moving objects	Vehicles	Vehicles, miners	Cages
Conductors	Pipes, wires, rails	Pipes, wires, rails	Wire ropes, pipes

The measurements were conducted in a vertical mine shaft in Hunan Province, China. The shaft can be considered a cylinder with a depth of 670 m and diameter of 4.5 m. The inner surface is made of concrete with roughness of 1–4 cm. An iron cage with a rectangular bottom of 3.8×1.8 m is placed in the center of the shaft, as shown in Figure 1, in which the marked dots (A/B/C) represent the antenna placement points. On the side of the cross-section, an iron balance weight is placed to balance the lifting moment by an opposite motion of the cage.

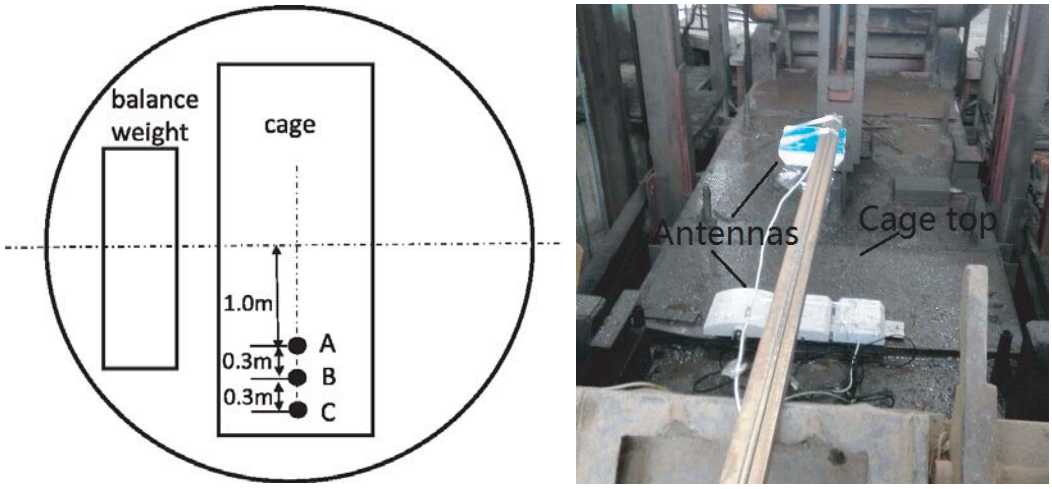

(a) (b)

Figure 1. Cross section of the shaft and antenna placement points. (a) Simplified graph. (b) Field photo.

2.2. Measurement Setup

Both narrowband and wideband measurements were conducted. Research has shown that antennas have an important influence on the channel characteristics in the confined space. A directional antenna was found to increase the coverage and decrease the delay spread obviously in such space [19, 20]. Thus, directional antennas were selected in both narrowband and wideband measurements. The main parameters of the antennas are given in Table 2. In the measurements, one antenna was put on the outside top of the cage and the other placed at the mouth of the shaft by a stick which was 1.5 m above the ground. No obstacle exists between the antennas during the measurements.

Table 2. Main parameters of the antennas.

Frequency	Gain [dBi]	Bandwidth [MHz]	Half-power beamwidth [°]
433 MHz	6	423 ∼ 443	H60/V60
900 MHz	7	790 ∼ 1020	H50/V50
2400 MHz	12	2300 ∼ 2500	H30/V30

Narrowband measurement setup is illustrated in Figure 2(a), in which the continuous wave technique was applied. A radio frequency signal source placed in the cage was used as the transmitter (Tx), and the handheld spectrum analyzer R&S FSH4 placed on the ground was used as the receiver (Rx). The transmitting frequency was set to 433, 900, 2400 MHz, respectively, with a transmitting power of 9 dBm. The antennas were linked to the Tx and Rx by 3-meter RF cables. The Rx was linked to the laptop by Ethernet, thus the laptop could control the Tx and acquire the measured data by an FSH4 View software. The laptop was also connected to the programmable logic controller (PLC) of the mine hoist, thus the depth data of the cage could be acquired by a WinCC software, then the Tx-Rx distance was calculated. During the measurement, the cage moved at a speed of 0.2 m/s. The receiving points were spaced 0.5 m, and four measuring data were obtained at each point, then averaged to reduce the effect of the random error. Measurements of different combinations of antenna positions were conducted, and the alternative placement points (A/B/C) are shown in Figure 1.

The sweep frequency technique was applied in the wideband measurements. In this technique, a

vector network analyzer (VNA) is used. The swept frequency signal transmits from one port of the VNA, then goes through the wireless channel and arrives at the other port of the VNA. Thus the frequency domain parameter S_{21} was acquired. Considering that the measured data contain device effect, a calibration was implemented to remove the effect of the system [21]. Then the time domain channel impulse responses (CIRs) could be obtained through a complex inverse Fourier transform (IFT) technique.

Wideband measurements were conducted only at 900, 2400 MHz, considering that the wireless systems at 433 MHz are mostly narrowband ones. The measurement setup is shown in Figure 2(b). The R&S FSH4 could also be used in a VNA mode. The two ports of the VNA were linked to the antennas through a 40-m cable and a 3-m RF cable, respectively, which limited the measuring range to less than 40 m. The center frequencies were set to 900 and 2400 MHz, respectively, with a bandwidth of 200 MHz. The bandwidth was divided into 631 points, resulting in a time resolution of 5 ns and time range of 3 μs. The sweep time was set to 20 ms, thus the channel could be considered quasi-static. The antennas were both placed at point A. The receiving points were spaced 0.3 m. The measured data and depth data were both stored in the laptop, as that in the narrowband measurement.

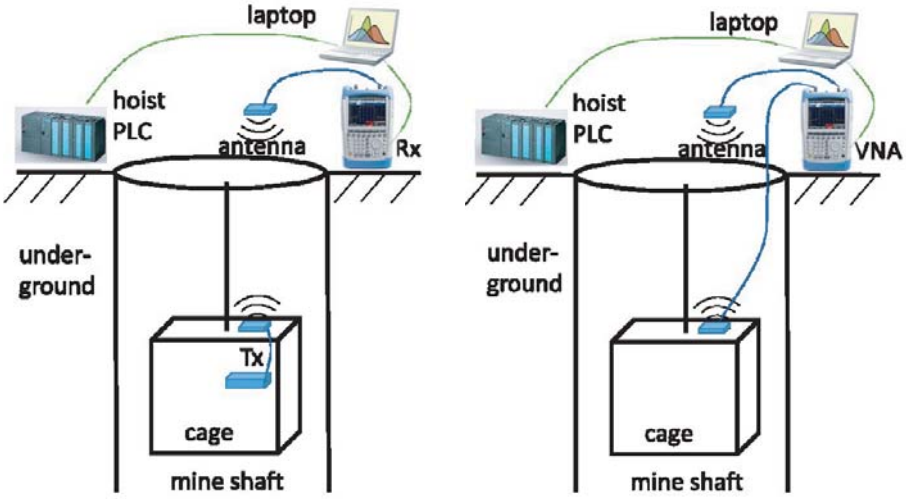

Figure 2. Radio channel measurement setups. (a) Narrowband measurement setup. (b) Wideband measurement setup.

3. RESULT AND DISCUSSIONS

3.1. Narrowband Results

3.1.1. Effect of Frequency on Path Loss

Path loss was extracted from the narrowband measured data. Figure 3 illustrates the relationship between the path loss and Tx-Rx distance when the antennas were both placed at point A. Results show that in the beginning region, the path loss at a lower frequency is smaller, similar to that in free space. However, the attenuation rate at a lower frequency is much larger. As the distance increases, the attenuation at the lower frequency catches up and exceeds that of the higher frequency, different from that in free space.

The common exponential path loss model is described as:

$$PL(d) = PL(d_0) + 10n \times \log(d/d_0) + X_\sigma, \tag{1}$$

where n is the path loss exponent, d_0 the reference distance, and X_σ a Gaussian random variable with a zero mean value and a standard deviation of σ.

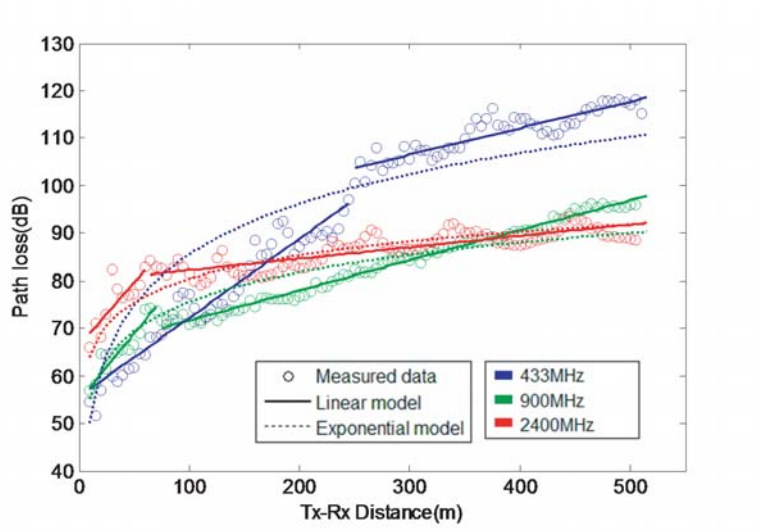

Figure 3. Path loss as a function of Tx-Rx distance.

The path loss exponent n was determined by least square regression analysis when $d_0 = 10\,\text{m}$. The results are presented in Table 3. It shows that the path loss exponents at 433, 900, 2400 MHz are much larger than that close to and smaller than that in free space (where n is equal to 2), respectively. It indicates that a higher frequency gets better coverage in a mine shaft environment, different from that in free space and similar to that in the straight tunnels [16]. Moreover, the waveguide effect was exhibited at 2.4 GHz since n is smaller than 2. As a matter of fact, if the omnidirectional antennas were applied, the path loss exponent would be expected to be smaller [22]. In lift shafts, the waveguide effect was also found to be one of the main propagation modes [23]. The waveguide effect could be excited by the straight, smooth walls and the longitudinal conductors such as the pipes.

Table 3. Parameters of the path loss model.

Frequency	PL (d_0) [dB]	n	σ [dB]
433 MHz	49.1	3.62	8.6
900 MHz	55.4	2.06	3.6
2400 MHz	64.3	1.67	2.7

Some measured path loss exponents in road/underground tunnels are listed in Table 4. The path loss exponent at 465 MHz in an underground tunnel is much larger than that in this paper at 433 MHz. The main reason is that the extra loss caused by the train is serious. Another measurement at 400 MHz in an underground road tunnel got an attenuation rate of approximately 13 dB/100 m [9], close to that in this paper. The path loss exponent at 900 MHz and 2400 MHz in this paper is similar to that in straight road tunnels and smaller than that in underground mine tunnels. It can be explained that in the underground mine tunnels with rough walls and irregular cross-sections, the rough loss and tilted loss are considerable [4].

The path losses at all frequencies obviously attenuate fast in the near region and slowly in the far region, similar to that in tunnels [11, 15]. It is because in the near region, higher modes which have high attenuation rates exist, while in the far region, the lower modes dominate.

The piecewise linear models for the path loss were also established, as shown in Table 5 and Figure 3, in which the breakpoints were determined adaptively according to the minimum-mean-error principle. The mean and standard values of the exponential model and linear model errors were calculated, as shown in Table 6. It shows the linear model fits better, especially for the lower frequency.

Table 4. Some measured path loss exponents in road/underground tunnels.

Frequency	n	Description	Research
465 MHz	9.72	Quasi-straight underground railway tunnel; Tx on the platform and Rx in the rare carriage of the train	[24]
900 MHz	2.0	Straight underground tunnels; high transmitter-high receiver combination	[12]
2.4 GHz	2.03, 2.05, 2.16	Straight underground mine tunnels	[13–15]
	1.58	Straight subway tunnel	[25]

Table 5. The piecewise linear model express for path loss.

	Near region	Far region	Breakpoint
433 MHz	$0.166d + 55.6$	$0.056d + 89.7$	245 m
900 MHz	$0.282d + 54.8$	$0.063d + 65.4$	70 m
2400 MHz	$0.265d + 66.3$	$0.024d + 79.8$	60 m

Table 6. Statistical values of model errors (exponential model/linear model).

	Mean (dB)	Standard deviation (dB)
433 MHz	1.50/−0.03	7.89/2.62
900 MHz	0.36/−0.01	3.59/1.04
2400 MHz	−0.04/0.08	2.65/2.17

3.1.2. Effect of Antenna Position on Path Loss

The antenna positions have been proved to have a significant impact on path loss in rectangular tunnels [12, 19, 20]. The alternative antenna positions are shown in Figure 1(a). Unfortunately, point B was unavailable for the cage antenna, limited by the field condition. The path loss was expressed as $PL(XY)$ in a case where the Tx, Rx antennas were placed at points X, Y, respectively.

Figure 4 illustrates the path losses of different antenna position combinations. In Figs. (a)∼(c), when the Tx antenna was placed at point A, the path losses at the different Rx antenna positions at the frequency of 433, 900, 2400 MHz are shown, respectively.

The path loss exponents of different antenna position combinations are shown in Table 7. It can be seen that $PL(AA) < PL(AB) < PL(AC)$ at all three frequencies.

Table 7. Path loss exponents of different antenna position combinations.

Case	433 MHz	900 MHz	2400 MHz
AA	3.62	2.06	1.64
AB	3.75	2.08	1.72
AC	3.80	2.31	1.81

Moreover, the path loss curves in different combinations at the same frequency are very similar, while they are quite different in the same combination at different frequencies. It illustrates that the effect of frequency on path loss is much larger than that of antenna position.

In Figure 4(d), $PL(AA), PL(CA)$ and $PL(CC)$ at 2400 MHz are compared. It can be seen that

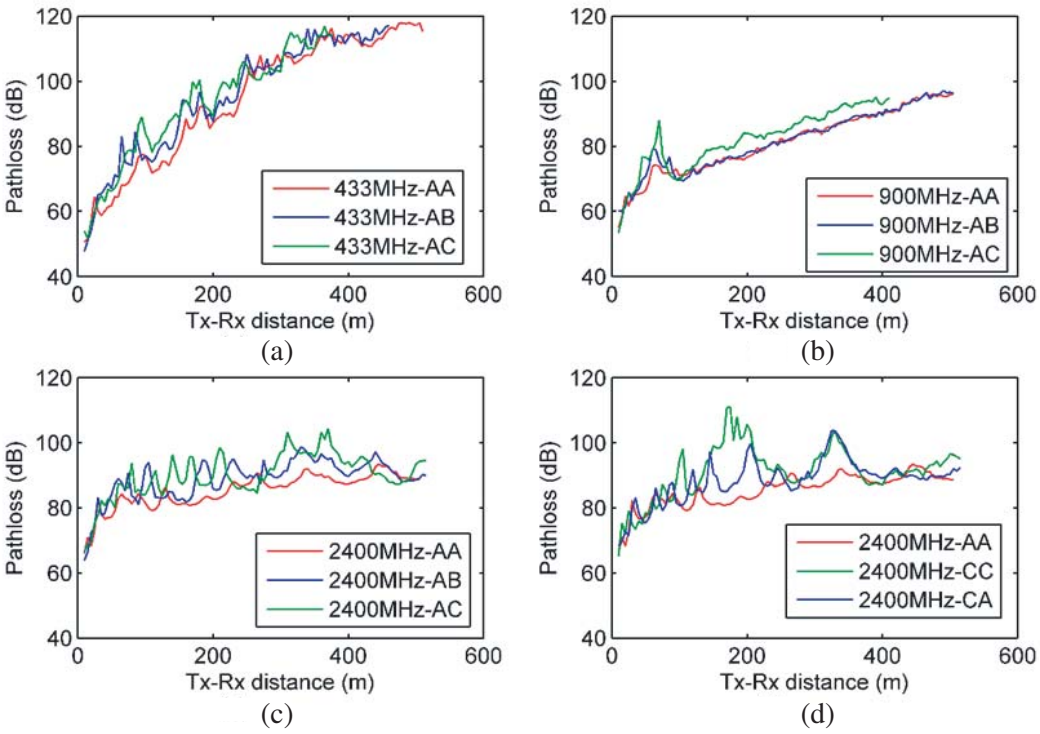

Figure 4. Path loss of different antenna position combinations.

$PL(AA) < PL(CA) < PL(CC)$, indicating that either the Tx or Rx antenna is close to the wall, and the path loss increases, similar to that in indoor corridor [12]. In addition, fluctuations of $PL(CA)$ and $PL(CC)$ are more severe than $PL(AA)$. It means that the off-center condition has a greater impact on the path loss than the alignment condition. Measurements at 433, 900 MHz have a similar situation. It is because when the antenna is close to the wall, a lot of energy will be transferred into higher order modes, which attenuates fast and fluctuates acutely because of the complex interactions [20]. Therefore, both Tx and Rx antennas are suggested to be placed close to the center of the cross-section.

3.2. Wideband Results

The wideband results are of great significance to select the optimal bit rate for a wireless system [26]. In a wideband system, attenuation, delay, and phase shift exist between the received and transmitted signals, characteristics of which can be described by the impulse response:

$$h(\tau) = \sum_{k=0}^{N-1} a_k \delta(\tau - \tau_k) e^{j\theta_k}, \tag{2}$$

where N is the number of multiple paths, δ the delta function, a_k the amplitude, τ_k the arrival time and θ_k the phase of the kth path, respectively.

Then the important mean and RMS delay spread parameters, which describe the time dispersion, are calculated by:

$$\overline{\tau} = \frac{\sum_k a_k^2 \tau_k}{\sum_k {a_k}^2}, \tag{3}$$

$$\tau_{rms} = \sqrt{\frac{\sum_k a_k^2 \tau_k^2}{\sum_k {a_k}^2} - \overline{\tau}^2}, \tag{4}$$

The wideband measured data were transferred to the time domain impulse responses by the complex IFT technology. A Hanning window was implemented to reduce the spectrum leakage. The delay

Table 8. Statistics of delay spread parameters (900 MHz/2400 MHz, [ns]).

	$\overline{\tau}$	τ_{rms}	$\tau_{\max}$
Mean	6.7/0.3	4.1/3.8	67.8/103.1
Standard deviation	10.3/0.3	1.9/2.5	35.2/58.7
Maximum	40.5/1.1	12.6/11.7	160/205

spread parameters were obtained by Equations (3)–(4). The noise floor threshold was determined by the average value of the CIR amplitude data after removing the maximum and minimum 25% ones [27]. The statistical values of the delay spread parameters are given in Table 8.

The mean values of the RMS delay spread at 900, 2400 MHz were calculated to be 4.1, 3.8 ns, respectively. At 900 MHz, the RMS delay spread was found less than 25 ns in empty tunnels [28], and the mean values were found 39 ns in an underground tunnel and 23 ns in indoor corridor environment [12]. At 2400 MHz, the mean values of the RMS delay spread in underground tunnels were found 27.4 [13], 6.3 [14], and 6.5 [15] ns. It can be seen that the measured data in this paper are smaller than that in most road or mine tunnels. The reason could be that directional antennas reduce the effects on the multipath significantly [19].

Figure 5 illustrates the RMS delay spread as a function of Tx-Rx distance. As the distance increases, the RMS delay spread increases in a short distance, then decreases to a small value in the far distance, at both 900 and 2400 MHz. The similar tendency was also observed in indoor [29] and tunnel [19] environments, but no obvious correlation was observed in underground mines [15]. In [17], a test of propagation when the train passes from the stain into the tunnel shows that the RMS delay spread also decreases to a very small value (2.6 ns at 980 MHz and approximately 0 ns at 2450 MHz) as the train goes into the deep-tunnel. The tendency could be explained by the multimode model, in which the delay spread depends on the significant modes as well as the path lengths. In the short distance, the lower and higher mode paths are both significant, and the difference of path lengths increases as the distance increases, resulting in an increase of delay spread. In far distance, the higher mode paths gradually disappear because of high attenuation, causing a decrease of the delay spread [5]. It shows that the tendency could be applied in the smooth-walled environments such as indoors, tunnels, and shafts, instead of the underground tunnels with rough walls and more random scatterings. Moreover, a small peak of RMS delay spread was observed at about 24 m, and the reason may be the reflections caused by the complex steel frame nearby.

The number of multipath components as a function of Tx-Rx distance is shown in Figure 6. The number is smaller than 8 at most locations for both 900 and 2400 MHz. However, the number in the far

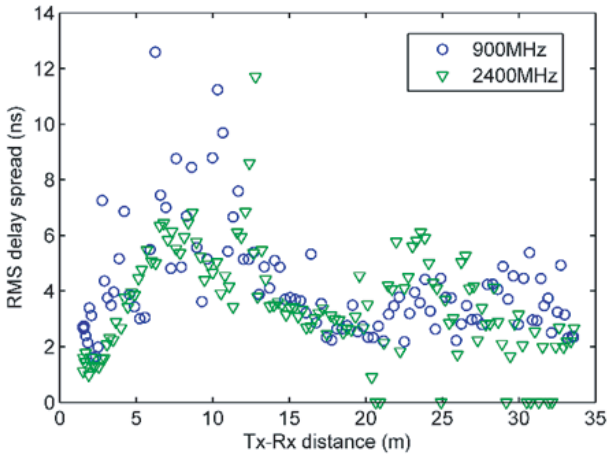

Figure 5. RMS delay spread as a function of Tx-Rx distance.

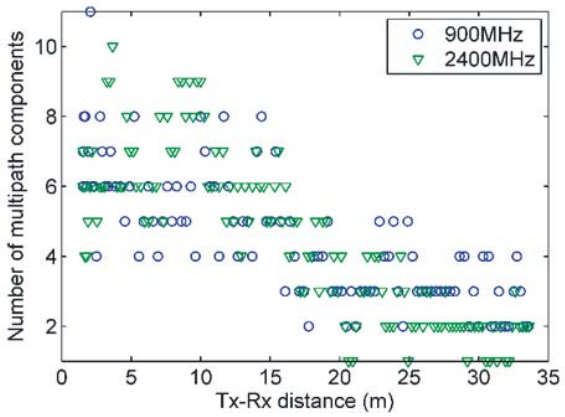

Figure 6. Number of multipath components as a function of Tx-Rx distance.

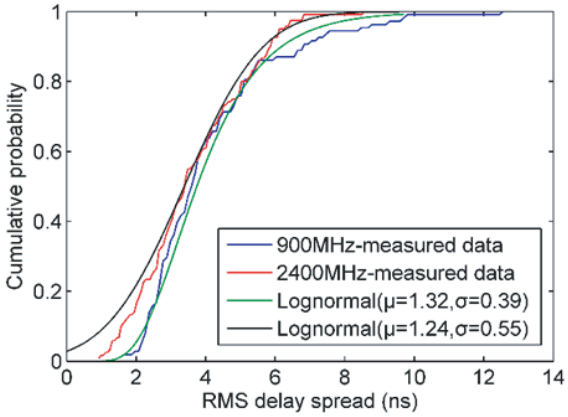

Figure 7. CDF of the RMS delay spread.

distance is obviously smaller than in the short distance, due to the disappearance of the higher modes, corresponding to the explanation of the RMS delay spread trend. A correlation analysis between the number and distance was applied to reveal the relationship between them. The Pearson correlation coefficients were calculated to be -0.77, -0.83 at 900 and 2400 MHz, respectively, meaning a strong negative correlation. Therefore, a small number of multipath components and a small delay spread are estimated beyond the measuring range.

Figure 7 illustrates the cumulative probability distribution functions (CDFs) of the RMS delay spread. It can be seen that the RMS delay spread is overall smaller at a higher frequency. For 90% measuring points, the RMS delay spread is found less than 6.9, 5.7 ns at 900 and 2400 MHz, respectively. In order to find which distribution represents the RMS delay spread best, the fitting curves following the Normal, Lognormal, Rician, Rayleigh and Weibull distributions were obtained, respectively; then the Kolmogorov-Smirnov (K-S) tests [14] were applied, and the p parameters were obtained, as shown in Table 9. Results demonstrate that lognormal distribution fits the experimental curves best.

Table 9. The p parameters in K-S tests of different distributions for the RMS delay spread.

	900 MHz	**2400 MHz**
Normal	0.087	0.351
Lognormal	0.362	0.683
Rician	0.083	0.670
Rayleigh	0.083	0.240
Weibull	0.138	0.674

4. CONCLUSIONS

Narrowband and wideband measurements were conducted at typical ultra-high frequencies of 433, 900, 2400 MHz in an actual mine shaft. To our knowledge, this is the first work focusing on the propagation in the mine shaft environment. The important parameters such as the path loss, delay spread and the number of multipath components were presented and compared with that in tunnel environments. Results show that the path loss exponents are larger than, approximate to and smaller than that in free space at 433, 900, and 2400 MHz, respectively. A waveguide effect exhibits at the high frequency. The piecewise linear model presents the path loss better than the exponential model, especially for the lower frequency. The effect of antenna positions on the path loss was investigated, showing that the path loss

increases as either the Tx or the Rx antenna is placed close to the wall. Moreover, the effect of antenna positions on path loss is much smaller than that of frequencies. The RMS delay spread is found less than 7 ns for most locations at both 900 and 2400 MHz, smaller than that in tunnel environments. In addition, it is smaller at the higher frequency. The relationship between the RMS delay spread and the distance was analyzed, showing that the RMS delay spread increases at the beginning then decreases to a small value as the distance increases. The distribution of the RMS delay spread was also investigated, indicating that the lognormal distribution fits well.

It would deepen our understandings of mine shaft channels and provide the basic parameters for the designers. Some suggestions could be given, for example: the frequency is suggested to be 2.4 GHz due to the small path loss and delay spread; the center position is suggested for the antenna placements due to the small path loss and fluctuation. More measurements in different shafts will be carried out to find sound shaft channel models in the future, such as the effect of shaft cross-section size on path loss and delay spread.

ACKNOWLEDGMENT

This research was funded by the National Basic Research Development Program of China (973 Program) grant number 2014CB049400.

REFERENCES

1. Ranjan, A., P. Misra, B. Dwivedi, and H. B. Sahu, "Studies on propagation characteristics of radio waves for wireless networks in underground coal mines," *Wireless Personal Communications*, Vol. 97, No. 12, 1–14, 2007.
2. Hrovat, A., G. Kandus, and T. Javornik, "A survey of radio propagation modeling for tunnels," *IEEE Communications Surveys & Tutorials*, Vol. 16, No. 2, 658–669, 2014.
3. Zhou, X., Z. Zhong, X. Bian, R. He, R. Sun, and K. Guan, "Measurement and analysis of channel characteristics in reflective environments at 3.6 GHz and 14.6 GHz," *Applied Science*, Vol. 7, No. 2, 165, 2017.
4. Sun, Z. and I. F. Akyildiz, "Channel modeling and analysis for wireless networks in underground mines and road tunnels," *IEEE Transactions on Communications*, Vol. 58, No. 6, 1758–1768, 2010.
5. Zhou, C., "Ray tracing and modal methods for modeling radio propagation in tunnels with rough walls," *IEEE Transactions on Antennas & Propagation*, Vol. 65, No. 5, 2624–2634, 2007.
6. Fono, V. A. and L. Talbi, "Modeling the effect of periodic wall roughness on the indoor radio propagation channel," *Progress In Electromagnetics Research M*, Vol. 49, 167–179, 2016.
7. Rana, M. M. and A. S. Mohan, "Segmented-locally-one dimensional FDTD (LOD-FDTD) method for large complex tunnel environments," *IEEE Transactions on Magnetics*, Vol. 28, No. 2, 223–226, 2012.
8. Zhang, Y. P., "Novel model for propagation loss prediction in tunnels," *IEEE Transactions on Vehicular Technology*, Vol. 52, No. 5, 1308–1314, 2003.
9. Hrovat, A., G. Kandus, and T. Javornik, "Four-slope channel model for path loss prediction in tunnels at 400 MHz," *IET Microwaves Antennas & Propagation*, Vol. 4, No. 5, 571–582, 2010.
10. Fan, J., S. Guo, X. Zhou, et al., "Faster-than-nyquist signaling: An overview," *IEEE Access*, Vol. 5, No. 99, 1925–1940, 2017.
11. Adewumi, A. S. and O. Olabisi, "Characterization and modeling of vegetation effects on UHF propagation through a long forested channel," *Progress In Electromagnetics Research Letters*, Vol. 73, 9–16, 2018.
12. Arslan, H. and S. Yarkan, "Statistical wireless channel propagation characteristics in underground mines at 900 MHz: A comparative analysis with indoor channels," *Ad Hoc Networks*, 2011.
13. Nerguizian, C., C. L. Despins, S. Affes, and M. Djadel, "Radio-channel characterization of an underground mine at 2.4 GHz," *IEEE Transactions on Wireless Communications*, Vol. 4, No. 5, 2441–2453, 2005.

14. Hakem, N., G. Delisle, and Y. Coulibaly, "Radio-wave propagation into an underground mine environment at 2.4 GHz, 5.8 GHz and 60 GHz," *The 8th European Conference on Antennas and Propagation*, 3592–3595, 2014.
15. Boutin, M., A. Benzakour, C. L. Despins, and S. Affes, "Radio wave characterization and modeling in underground mine tunnels," *IEEE Transactions on Antennas & Propagation*, Vol. 56, No. 2, 540–549, 2008.
16. González-Plaza, A., C. Calvo-Ramírez, C. Briso-Rodríguez, et al., "Propagation at mmW band in metropolitan railway tunnels," *Wireless Communications & Mobile Computing*, 1–10, 2018.
17. Zhang, L., C. Briso, J. R. O. Fernandez, J. I. Alonso, et al., "Delay spread and electromagnetic reverberation in subway tunnels and stations," *IEEE Antennas & Wireless Propagation Letters*, Vol. 15, No. 4, 585–588, 2016.
18. Hussain, I., F. Cawood, and R. V. Olst, "Effect of tunnel geometry and antenna parameters on through-the-air communication systems in underground mines: Survey and open research areas," *Physical Communication*, Vol. 23, 84–94, 2017.
19. Bashir, S., "Effect of antenna position and polarization on UWB propagation channel in underground mines and tunnels," *IEEE Transactions on Antennas & Propagation*, Vol. 62, No. 9, 4771–4779, 2014.
20. Li, D. and J. Wang, "Effect of antenna parameters on the field coverage in tunnel environments," *International Journal of Antennas and Propagation*, Vol. 2016, 1–10, 2016.
21. Varela, M. S. and M. G. Sanchez, "RMS delay and coherence bandwidth measurements in indoor radio channels in the UHF band," *IEEE Transactions on Vehicular Technology*, Vol. 50, No. 2, 515–525, 2001.
22. Dabin, J. A., N. Ni, A. M. Haimovich, et al., "The effects of antenna directivity on path loss and multipath propagation in UWB indoor wireless channels," *IEEE Conference on Ultra Wideband Systems and Technologies*, 305–309, 2003.
23. Mao, X. H. and Y. H. Lee, "Comparison of propagation along a lift shaft in two complex environments," *Progress In Electromagnetics Research B*, Vol. 36, 337–355, 2012.
24. Zhang, Y. P., Z. R. Jiang, T. S. Ng, and J. H. Sheng, "Measurements of the propagation of UHF radio waves on an underground railway train," *IEEE Transactions on Vehicular Technology*, Vol. 49, No. 4, 1342–1347, 2000.
25. Li, J., Y. Zhao, J. Zhang, et al., "Radio channel measurements and analysis at 2.4/5 GHz in subway tunnels," *China Communication*, Vol. 12, No. 1, 36–45, 2015.
26. Moreno, J., I. Val, A. Arriola, et al., "2.6 GHz intra-consist channel model for train control and management systems," *IEEE Access*, Vol. 5, 23052–23059, 2007.
27. Wu, X., Y. Shen, and Y. Tang, "Measurement and modeling of co-time co-frequency full-duplex self-interference channel of the indoor environment at 2.6 GHz," *Acta Electronica Sinica*, Vol. 43, No. 1, 1–6, 2015.
28. Zhang, Y. P. and Y. Hwang, "Characterization of UHF radio propagation channels in tunnel environments for microcellular and personal communications," *IEEE Transactions on Vehicular Technology*, Vol. 47, No. 1, 283–296, 1998.
29. Geng, S., J. Kivinen, and P. Vainikainen, "Propagation characterization of wideband indoor radio channels at 60 GHz," *IEEE International Symposium on Microwave, Antennas, Propagation and EMC Technologies for Wireless Communications*, 314–317, 2005.